Comparison of Measured Leakage Current Distributions with Calculated Damage Energy Distributions in HgCdTe

C. J. Marshall, P. W. Marshall, *Member, IEEE,* C. L. Howe, *Student Member, IEEE,* R.A. Reed, *Member, IEEE,* R. A. Weller, *Senior Member, IEEE,* M. Mendenhall, A. Waczynski, R. Ladbury, T. T. Jordan, and B. Fodness

Abstract—**This paper presents a combined Monte Carlo and analytic approach to the calculation of the pixel-to-pixel distribution of proton-induced damage in a HgCdTe sensor array and compares the results to measured dark current distributions after damage by 63 MeV protons. The moments of the Coulombic, nuclear elastic and nuclear inelastic damage distribution were extracted from Monte Carlo simulations and combined to form a damage distribution using the analytic techniques first described in [1]. The calculations show that the high energy recoils from the nuclear inelastic reactions (calculated using the Monte Carlo code MCNPX [2]) produce a pronounced skewing of the damage energy distribution. The nuclear elastic component (also calculated using the MCNPX) has a negligible effect on the shape of the damage distribution. The Coulombic contribution was calculated using MRED [3,4], a Geant4 [4,5] application. The comparison with the dark current distribution strongly suggests that mechanisms which are not linearly correlated with nonionizing damage produced according to collision kinematics are responsible for the observed dark current increases. This has important implications for the process of predicting the on-orbit dark current response of the HgCdTe sensor array.**

I. INTRODUCTION

MANY emerging space astronomy programs will perform their science using infrared detectors in order to study the early Universe as well as Earth and planetary sciences, and the infrared bands are also important in military applications. Although we have observed hot pixel formation in proton-irradiated Rockwell IR hybrid detectors to be used in the James Webb Space Telescope [7], we do not as yet understand the mechanism producing the hot pixels in HgCdTe. As a result we are unable to predict hot pixel formation on orbit. The purpose of this paper is to predict the proton-induced displacement damage distributions in $Hg_{0.7}Cd_{0.3}Te$ based on collision kinematics to see if they predict the observed dark current distribution.

In the case of Si sensors (including charge couple devices, active pixel sensors and charge injection devices) measurements show that the dark current distributions are often well explained by the damage distributions calculated based on collision kinematics [1,8-11]. Damage distributions were first calculated analytically by Marshall et al. in 1990 with good agreement obtained for dark current distributions produced by 12 MeV protons in Si charge injection devices. At 63 MeV the data indicated less variance in the measured distribution than in the damage energy calculation, a result also found by Hopkinson et al. at 100 MeV in Si charge coupled devices (CCDs). Using the Monte Carlo code CUPID [12] Dale et al. showed that this result followed because the recoil ranges were comparable to the size of the dark current sensitive volume. In the limit of bulk material, both the analytic and the CUPID Monte Carlo approaches are in good agreement. As sensitive volumes shrink and incident proton energies increase, the ranges of the spallation recoil fragments approach the smallest dimension of the microvolume, and the pixel-to-pixel damage variance are best calculated using methods which track the damage deposition along the recoil atom pathlengths . In this regime, a Monte Carlo approach is well suited to describe the damage energy distribution.

Nevertheless, in some cases the Si dark current distributions cannot be described using collision kinematics. This has been attributed to hot pixel formation from electric field enhanced emission [e.g. 10, 13-16]. It is important to distinguish the two scenarios because in order to predict the hot pixel populations, one needs to understand whether they are formed by extraordinarily large damage regions from inelastic reactions in the pixel or by electric field enhanced emission which appears to follow from small damage regions in very small microvolumes filling only a tiny fraction of the pixel's volume. In the later case the hot pixel population may be expected to follow the Coulomb cross section [16, 17].

Manuscript received June 20, 2006. The authors appreciate funding from the NASA Electronics and Packaging Program (NEPP), the DTRA Radiation Hardened Microelectronics Program and the James Web Space Telescope project. The authors also appreciate useful discussions with John Hubbs from Ball Aerospace.

C. J. Marshall and R. Ladbury are with the NASA-GSFC, Greenbelt, MD 20771 USA (corresponding author phone: 434-376-3402; fax: 703-991-6115; e-mail: cmarshall2@aol.com).

P. W. Marshall is a consultant, Brookneal, VA 24528 USA.

R. A. Reed, C. Howe, B. Weller, and M. Mendenhall are with Vanderbilt University, Nashville, TN 37235 USA.

A. Waczynski is with Global Science and Technology, Greenbelt, MD 20771 USA.

T.M. Jordan is with EMPC, Gaithersburg, MD 20885 USA.

B. Fodness is formerly a NASA/GSFC support contractor with SGT, Inc., Greenbelt, MD 20771

II. The Experiment

We use previously measured dark current distribution of a Rockwell H-2RG which is a hybrid device with a 2k x 2k format and 18 micron pixel pitch. It incorporates a software configurable silicon readout circuit bump bonded to a HgCdTe detector array optimized for the JWST NIR (0.6 – 5 μm) spectral range. Details of the experiment can be found in [7] but key details are provided.

An engineering grade device was employed and displayed a number of cosmetic defects and 'hot' pixels that did not meet the stringent JWST flight FPA operability requirements going into our test. A subset of ~266,000 pixels were extracted that were deemed to be "good" pixels as will be described in the full paper. The detector held at 37 K and irradiated with 63 MeV protons to a 5 krad(Si) level which corresponds to a fluence of 3.7e10 cm^{-2}. The dewar was maintained at temperature while being transported back to the NASA Ames laboratory and measurements were taken after residual radioactivity from the proton exposure had mostly decayed. Residual activity and cosmic ray effects were filtered out as described in [7].

III. Damage Energy Distribution Calculations

In this section we follow the method described in [1] to calculate the damage energy distribution for 63 MeV protons on $Hg_{0.7}Cd_{0.3}Te$. The first step in the calculation of damage energy distributions is to calculate the interaction cross sections (σ), as well as the first and second moments of the $Hg_{0.7}Cd_{0.3}Te$ damage energy distributions due to Coulombic, nuclear elastic and nuclear inelastic interactions respectively. The first moment corresponds to the mean damage energy, (μ) and the second moment is the associated variance, (var). These means and variances correspond to the probability density function (pdf) governing the likelihood of a particular recoil energy resulting from a given proton- $Hg_{0.7}Cd_{0.3}Te$ interaction.

The next step is to calculate the average number of inelastic recoils per pixel. For the sensitive volumes (V_{pixel}) and fluences (Φ) of interest the average number of inelastic recoils per pixel ($N_{recoils}$) is small therefore there is a discrete Poisson distribution of recoils throughout the array.

$$P(x,\lambda) = \frac{(e^{-\lambda} \bullet \lambda^{x})}{x!}$$ where x = 0,1,2,... inelastic recoils per pixel. λ is the average number of recoils per pixel and is given by $N_{recoils} = \sigma*\Phi*\rho*V_{pixel}*N_{avogadro}/A$ where ρ is the HgCdTe density and A is the gram atomic weight of $Hg_{0.7}Cd_{0.3}Te$. Note that $\sum P(x,\lambda) = 1$.

Next one calculates the single event probability function (SEpdf) for inelastic nuclear reactions as approximated by a 2 parameter (μ and var) gamma distribution. (This function is also normalized to unit area.) Next one calculates the N-fold convolution of the SEpdf with itself to get the pdf for a pixel with N inelastic recoils. This is done for N = 2, 3, 4, etc, up to the maximum N expected to occur for the given population of pixels. Each of these distributions is convolved with the Coulombic distribution corresponding to the mean Coulomb damage energy per pixel. In addition, we determined the pixel-to-pixel variation in Coulomb damage and included this variance with the Poisson dominated variance in the incident particle fluence which was by far the dominant term. This gives us confidence in assuming a Gaussian form for the distribution of Coulomb damage throughout the array.

Finally, we weight each of these distributions with the Poisson probability for N (inelastic) recoils in a pixel and then sum them to arrive at the damage energy distribution corresponding to the pixel volumes (assumed 10 micron thickness) and fluence chosen. (Note that the nuclear elastic component has been ignored. We will justify this later in the next section.)

A. Material and Recoil Spectrum Parameters

The $Hg_{0.7}Cd_{0.3}Te$ has a density of 7.41 g/cm^3 and a gram molecular weight of 151 g. The pixel area is 18 μm by 18 μm and the epi layer is ~10 μm deep. From measurements on other HgCdTe detectors we expect the diffusion length to be at least 10 μm so dark current should be collected from the entire pixel volume. The volume and density are large enough so that we do not expect the ranges of the recoils to be long compared to the volume dimensions so the analytic approach should offer a valid approximation.

The results for the recoil spectrum parameters are shown in Table 1, along with the MRED [3,4] results for the Coulomb parameters in the units indicated. In the future, we plan to develop MRED for a more comprehensive and general solution but for now we are using it for a point solution for the case of 3.7 x 10^{10} cm^{-2} 63 MeV protons on the pixel geometry cited (i.e. 1.2 x 10^5 protons/pixel). The nuclear elastic component (calculated using the Monte Carlo code MCNPX [2]) has a negligible effect of the shape of the damage distribution. We can see from the table that the mean recoil energy and variance are an order of magnitude below that of the inelastic interactions. As can be seen from Figure 1, the nuclear elastic contribution to the nonionizing energy loss rate (NIEL) is negligible over the entire proton energy range of interest.

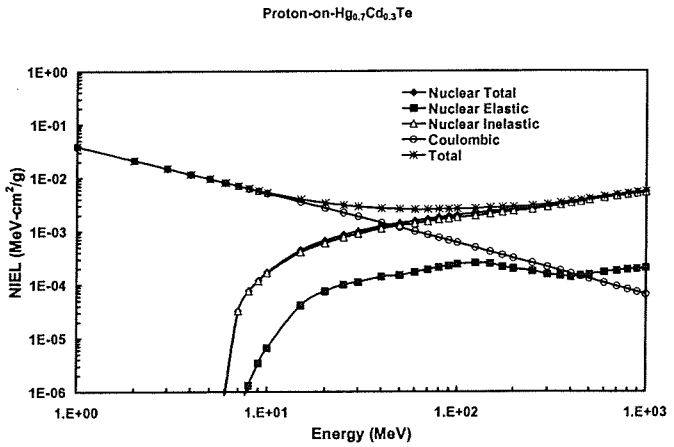

Figure 1 Proton NIEL in $Hg_{0.7}Cd_{0.3}Te$ as calculated in [18]. Note that the NIEL is very insensitive to the exact stoichiometry.

TABLE 1

Proton Nuclear Reactions on HgCdTe x=0.3

Proton Energy (MeV)	Cross Section (barns)	Mean Recoil Energy (MeV)	Mean Damage Energy (MeV)	Variance of Damage Energy $(MeV)^2$
Nuclear Elastic Reactions				
63	0.4984	0.0402	0.0254	6.85E-03
Nuclear Inelastic Reactions				
63	1.599	0.3721	0.2086	7.15E-02
Coulombic Interactions				
63			0.734*	9.60E-13**

*MeV per pixel with incident 63 MeV proton fluence of 3.7×10^{10} cm^{-2}.
** MeV^2 per pixel with a 63 MeV proton fluence of 3.7×10^{10} cm^{-2}.

The method used to compute the nuclear contribution to NIEL and the associated variance is based on the thin target approximation using MCNPX and a methodology developed by Jun [19]. A thin cylindrical slab of the material of interest with a normalized density of 0.01 atoms/barn-cm was modeled, and a simulated pencil beam of protons penetrates the material. The model considers a simulated pencil beam of protons normally incident on a thin, solid cylindrical disk. Using the damage energy tally, the history tape written by MCNPX was analyzed to calculate the mean damage energy per source particle, T_{dam}, which is the nonionzing portion of energy deposited (i.e. after application of the Lindhard partition function). Then, NIEL is calculated by: $S_{NIEL} = \left(\frac{N}{A}\right)\frac{T_{dam}}{(N_v \cdot x)}$ where N is Avogadro's number, A is the gram atomic weight of the target material, N_v is the atom density and x is the target thickness. By using MCNPX, we were able to compute the nuclear contributions to the proton NIEL for each material and then superimpose them to arrive at the NIEL for the $Hg_{0.7}Cd_{0.3}Te$. The production of displaced atoms is dominated by the Coulombic interactions below 10 MeV, while the nuclear collisions (particularly the nuclear inelastic) take over at energies exceeding 30-50 MeV. For the Coulombic NIEL shown in figure 1, the calculation was done analytically using the ZBL method. This analytic approach provides the mean, but not the variance for Coulomb scattering events. Using the history tape out of MCNPX we were also able to compute the variance of the damage energy as seen in Table 1.

We arrived at the distribution describing Coulomb damage based on the mean damage energy deposited in a large number of Monte Carlo runs (using MRED [3,4]]) for the pixel geometry and proton fluence of 3.7×10^{10} cm^{-2} 63 MeV protons. It is significant to note that the mean damage energy per pixel calculated using the NIEL value in figure 1 agrees to within 17% with the value obtained using the GEANT4 Monte Carlo runs. The variance expressed in the table has also been determined from the Monte Carlo runs. To properly incorporate variances due to kinematic considerations for the purpose of comparing damage distributions with measured dark current data we must also include a variance describing the measured distribution seen in the pre-irradiation dark current data. From figure 2 we note that the pre-rad distribution appears approximately Gaussian and has a mean near zero electrons per second. The variance in this Gaussian is not fully understood but we presume it to be influenced by the pixel-to-pixel fluctuations, noise from the array and readout electronics, thermal control fluctuations, and characteristics of the readout algorithm. After consideration of all the terms influencing the variation in pixels receiving only Coulomb damage, we discover that the variance representing the pre-irradiation measurement of the dark current is dominant (even being larger than the Poisson variation in the incident particle fluence noted earlier.)

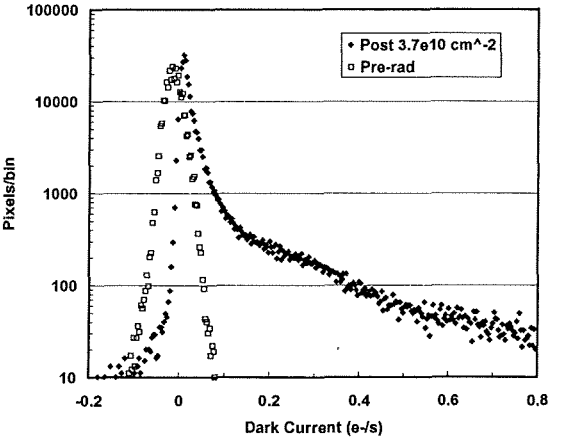

Figure 2 Measured dark current distribution for 266,000 $Hg_{0.7}Cd_{0.3}Te$ pixels before irradiation and after irradiation with 3.7×10^{10} cm^{-2} 63 MeV protons.

B. Calculated Damage Distributions

The calculated damage distribution is shown in Figure 3, which shows the distribution of pixels with elastic damage plus 0, 1, 2, etc. inelastic interactions. The average number of inelastic collisions per pixel was ~5, and the maximum number of inelastic recoils expected per pixels is 18 for our fluence and pixel population. As one can see, the inelastic collisions are responsible for the skewness in the distribution. The shape of the distribution is also significantly impacted by the camera response function which we noted dominates the form of the distribution representing the Coulombic contribution and is present in all measurements, but negligible in comparison to the damage energy variance where inelastic collisions are concerned. (Recall that the Coulombic variance is extremely small.)

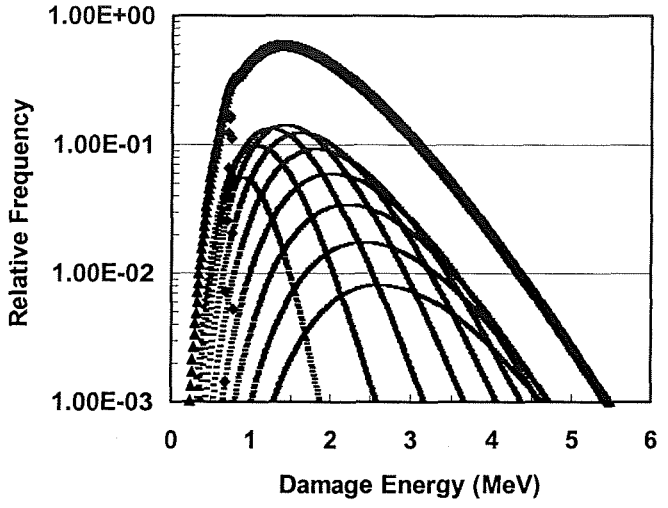

Figure 3 Calculated damage energy distribution for 266,000 $Hg_{0.7}Cd_{0.3}Te$ pixels irradiated with 3.7e10 cm^{-2} 63 MeV protons. Below the summed damage distribution we show the Poisson weighted damage distributions for the pixels with only Coulomb events (diamonds), and the pixels with Coulomb events plus 1,2,3...10 inelastic interactions per pixel. Note that a pixel may contain up to 18 inelastic interactions.

IV. Results and Summary

The measured dark current histogram for 266,00 selected pixels is shown in figure 2 along with the pre-irradiation histogram. In [5], the slight median shift was not investigated, and hence was not presented as necessarily real. Recently we have re-analyzed this data and do find a small shift in the median dark current after irradiation to 3.7 x 10^{10} cm^{-2} 63 MeV protons. It is apparent that the calculated damage distribution does not predict the measured dark current distribution which indicates that some other mechanism than collision kinematics is also responsible for the high dark current pixels. This makes an on-orbit prediction of the dark current problematic and the NIEL correlation does not appear to hold. Measurements at 8 MeV are planned to see if the high dark current pixels correspond to the Coulombic portion of the NIEL which would be the case if electric field enhanced emission is responsible as has been seen in Si.

References

[1] P. W. Marshall, C. J. Dale and E. A. Burke, "Proton-induced displacement damage distributions and extremes in silicon microvolumes," *IEEE Trans. on Nucl. Sci.*, Vol. 37, pp. 1776-1783, December 1990.

[2] "MCNPX User's Manual: Version 2.4.0," LA-CP-02-408, Los Alamos National Lab, September 2002.

[3] H. Mendenhall and R.A. Weller, "An algorithm for computing screened Coulomb scattering in Geant4," Nuclear Instruments and Methods A Vol. 227, pp. 420-430, 2005.

[4] R.A. Weller, M.H. Mendenhall, and D.M> Fleetwood, "A screened Coulomb scattering module for displacement damage computations in Geant4," IEEE Trans. Nucl. Sci, Vol.. 51, pp. 3669-3678, 2004.

[5] S. Agostinelli et al., "Geant4 –A simulation toolkit," Nucl. Instrum. Meth. Phys. Res., Vol. A 506, pp. 250-303, 2003.

[6] Geant4 [online]. Available: http://geant4.web.cern.ch/geant4

[7] M.E. McKelvey, K.A. Ennico, R.R. Johnson, P.W. Marshall, R.E. McMurray Jr., C.R. McCreight, J.C. Pickel and R.A. Reed, "Radiation environment performance of JWST prototype FPAs," SPIE Proceedings, Focal Plane Arrays for Space Telescopes, Vol. 5167, pp.223-234, 2003.

[8] G.R. Hopkinson, "Cobalt-60 and Proton Radiation Effects on Large Format, 2-D, CCD Arrays for an Earth Imaging Application," IEEE Trans. Nucl. Sci., Vol. 39, No. 6, pp. 2018-2025, 1992.

[9] M.S. Robbins, "High-Energy Proton-Induced Dark Signal in Silicon Charge Coupled Devices," IEEE Trans. Nucl. Sci., Vol. 47, No. 6, pp. 2473-2479, 2000.

[10] J. Bogearts, B. Dierickx, and R. Mertens, "Enhanced Dark Current Generation in Proton-Irradiated CMOS Active Pixel Sensors, Trans. Nucl. Sci., Vol. 49, No. 3, pp. 1513-1521, 2002.

[11] R. Germanicus, S. Barde, L. Dusseau, G. Rolland, C. Barillot, F. Saigne, R. Ecoffet, P. Calvel, J. Fequet, and J. Gasiot, "Evaluation and Prediction of the Degradation of COTS CCD Induced by Displacement Damage," IEEE Trans. Nucl. Sci., Vol. 49, No. 6, pp. 2830-2835, 2002.

[12] C.J. Dale, L. Chen, P.J. McNulty, P.W. Marshall, and E.A. Burke, "A comparison of Monte Carlo and analytic treatments of displacement damage in Si microvolumes," IEEE Trans. Nucl. Sci., Vol. 41, No. 6, pp. 1974-1983, 1994.

[13] P.W. Marshall, C.J. Dale, E.A. Burke, G. P. Summers, and G. E. Bender, "Displacement Damage Extremes in Silicon Depletion Regions," IEEE Trans. Nucl. Sci., Vol. 36, No. 6, pp. 1831-1839, 1989.

[14] J.R. Srour and R.A. Hartman, "Enhanced Displacement Damage Effectiveness in Irradiated Silicon Devices," IEEE Trans. Nucl. Sci., Vol. 36, No. 6, pp. 1825-1830, 1989.

[15] I.H. Hopkins and G.R. Hopkinson, "Further Measurements of Random Telegraph Signals in Proton-Irradiated CCDs," IEEE Trans. Nucl. Sci., Vol. 42, No. 6, pp. 2074-2081, 1995

[16] C.J. Marshall, P.W. Marshall, A. Waczynski, E.J. Polidan, S.D. Johnson, R.A. Kimble, R.A. Reed, G. Delo, D. Schlossberg, A.M. Russell, T. Beck, Y. Wen, J. Yagelowich, R.J. Hill, "Hot pixel annealing behavior in CCDs irradiated at -84°C," IEEE Trans. Nucl. Sci., Vol. 52, No. 6, pp. 2672-2677, 2005.

[17] P. W. Marshall, C. J. Dale, E. A. Burke, G. P. Summers, and G.E. Bender, "Displacement Damage Extremes in Silicon Depletion Regions," IEEE Trans. Nucl. Sci., Vol. 36, No. 6, pp. 1831-1839, 1989.

[18] B.C. Fodness, P.W. Marshall, R.A. Reed, T.M. Jordan, J.C. Pickel, I. Jun, M.A. Xapsos, E.A. Burke and R. Ladbury, "Monte Carlo Treatment of Displacement Damage in Bandgap Engineered HgCdTe Detectors," Proceedings of the 7th European Conference on Radiation and its Effects on Components and Systems, pp. 479-485, 2003.

[19] I. Jun, M.A. Xapsos, S.R. Messenger, E.A. Burke, R.J. Walters, G.P. Summers and T.M. Jordan, "Proton NonIonizing Energy Loss (NIEL) for device applications," presented at IEEE NSREC 2003.